Environ Earth Sci (2016) 75:1375
DOI 10.1007/s12665-016-6114-3

ORIGINAL ARTICLE

Magnetic characteristics and trace elements concentration in soils from Anthemountas River basin (North Greece): discrimination of different sources of magnetic enhancement

E. Aidona[1] · H. Grison[2] · E. Petrovsky[2] · N. Kazakis[3] · L. Papadopoulou[4] · K. Voudouris[3]

Received: 27 August 2015 / Accepted: 23 September 2016 / Published online: 19 October 2016

Abstract The magnetic minerals (e.g., iron oxides) that are present in soils can be easily identified by using rock-magnetic techniques. Increased magnetic susceptibility of soils may reflect particles rich in iron oxides of anthropogenic, lithogenic, and pedogenic origin. Therefore, reliable discrimination of these sources is required, especially in areas where neither of them is dominant. The aim of the present study is to assess the lithogenic and anthropogenic contributions to iron-oxide mineralogy of soils in the area of the Anthemountas River basin in the southeast part of Thessaloniki city. Previous investigations within the study area, based on spatial distribution of magnetic susceptibility, revealed the presence of two magnetically enhanced regions. Therefore, the present study is focused on these two areas, in order to characterize the origin of magnetic enhancement. Detailed magnetic analyses include properties reflecting the type, concentration, and relative grain-size distribution of magnetic particles. Moreover, trace element concentration is determined with an aim to establish the link between low-field mass-specific magnetic susceptibility and concentration of Fe, Cr, Ni, Mn, Pb, Zn, and Ti. These findings are supported by descriptions of the micromorphology performed by scanning electron microscopy and determination of elemental composition by energy-dispersive spectrometer analyses in selected points. Finally hierarchical cluster analysis is applied to classify the soil samples into appropriate groups according to their magnetic properties. The results reveal that magnetic measurements provide a useful tool for the discrimination between different magnetic sources responsible for the enhancement of magnetic susceptibility in soils. Low-field mass-specific magnetic susceptibility reflects increased concentration of trace elements, while its combination with other magnetic measurements clearly differentiates the origin of magnetic enhancement in both parts of the study area.

Keywords Magnetic susceptibility · Day plot · Trace elements · Pollution · Greece

✉ E. Aidona
aidona@geo.auth.gr

[1] Department of Geophysics, School of Geology, Aristotle University of Thessaloniki, 54124 Thessaloníki, Greece

[2] Institute of Geophysics CAS, Bocni II/1401, 14131 Prague 4, Czech Republic

[3] Laboratory of Engineering Geology and Hydrogeology, School of Geology, Aristotle University of Thessaloniki, 54124 Thessaloníki, Greece

[4] Department of Mineralogy, School of Geology, Aristotle University of Thessaloniki, 54124 Thessaloníki, Greece

Introduction

Natural iron-bearing minerals are sensitive to a range of environmental processes, making magnetic measurements extremely useful proxies for the detection of different factors influencing the environment. Techniques used for measuring magnetism of soil minerals primarily include the measurement of magnetic susceptibility (volume- and mass-specific magnetic susceptibility κ [dimensionless] and χ [m^3/kg], respectively) and induced and remanent magnetization (A/m). The main advantage of these methods is their sensitivity—magnetic susceptibility and magnetization can detect extremely small amounts of ferrimagnetic iron oxides (magnetite and maghemite); the main magnetic minerals responsible for enhancement of the magnetic susceptibility in soils (e.g., Mullins 1977).

Dearing (1994) reported that a small quantity of magnetite (0.01 %), in typical soil magnetic populations, contributes about 85 % to the total magnetic susceptibility. Magnetic minerals present in soils could be derived from the parent rocks (lithogenic origin), from anthropogenic activities, or be the result of pedogenic processes (e.g., Maher 1986). The total magnetic signal is therefore the result of different magnetic contributions.

Magnetic susceptibility reflects the ease with which a material is magnetized and is expressed as the ratio of the induced magnetization acquired by the application of a weak magnetic field to this applied field. Magnetic susceptibility has become the most frequently used magnetic soil property (for review see, e.g., Thompson and Oldfield 1986; Verosub and Roberts 1995; Liu et al. 2012). During the last several decades, magnetic susceptibility has been consistently used for the detection of environmental pollution of soils, sediments, and dusts. Several studies have been performed, demonstrating the enhancement of magnetic susceptibility in industrial and urban areas or along highways (e.g., Strzyszcz 1993; Scholger 1998; Petrovsky et al. 1998, 2000; Kapicka et al. 2001; Lecoanet et al. 2001; Boyko et al. 2004; Jordanova et al. 2004, 2014; Lu and Bai 2006).

One of the main questions which arise is the possibility to determine the contamination sources and to distinguish their influence (lithogenic, anthropogenic, and pedogenic) on the magnetic susceptibility of soils. Several authors have suggested various guidelines for the magnetic discrimination based either on magnetic susceptibility measurements along vertical profiles (Magiera et al. 2006) or/and the application of different statistical methods in large databases (Hanesch et al. 2007) or on the examination of additional magnetic properties (Fialova et al. 2006). Interpretation of magnetic data can be influenced by the choice of the sampling density (scale) of magnetic susceptibility measurements (Magiera and Zawadzki 2007). These authors pointed out that, in the case of low susceptibility values, the density of measured points should not be too high, whereas for the case of high susceptibility values where different contributions are expected, measurements over a denser measurement grid are required. Moreover, the influence of soil use (forest or arable land) has to be considered as well.

Despite this large development, only a few studies have been performed in Greece during the last decades (Scoullos et al. 1979; Sarris et al. 2009; Zananiri et al. 2010; Botsou et al. 2011). Recently, Aidona et al. (2013) presented the spatial distribution of magnetic susceptibility data from the broader area of Thessaloniki City in the Anthemountas River basin. In Aidona et al. (2013) two magnetically enhanced areas were identified. The main target of the present work is to extend the results of the previous study and investigate in detail the origin of the different magnetic contributions responsible for the enhancement of the magnetic susceptibility in this area. The study is based on (1) determination of magnetic properties, represented by the hysteresis and remanence data and by thermomagnetic curves; (2) geochemical analyses, represented by concentration of trace elements; and (3) detailed electron microscopy observations of magnetic minerals.

Materials and methods

Study area

The study area is located in the Anthemountas River basin in northern Greece, at the eastern part of the Thermaikos Gulf. It covers an area of 374 km^2 with high hills of semi-mountainous relief, according to Dikau's (1989) classification.

The geological formations of the area belong to three major geotectonic zones: the Serbo-Macedonian massif, the Circum-Rhodope, and the Paeonian (Mountrakis 1985). Hence, a variety of sedimentary and metamorphic formations are detected. The sedimentary formations are placed mainly in lowlands and consist of Quaternary and Neogene deposits. The Quaternary sediments are alluvial deposits (sands, gravels, and clays) and terrace systems (sands, pebbles, gravels, and clays), located in the western and the eastern part of the basin, respectively. The Neogene sediments are mainly located in the southern part of the area and are comprised of sandstone-marls (sandstones, marls, sands, and gravels), red-clays (clay with sand lenses) and conglomerate series (conglomerates, gravels, sands). The mountainous parts of the basin consist of Mesozoic ophiolitic, crystalline, and carbonate rocks. These carbonate rocks (Triassic limestones) are located in the south-center part of the basin. The ophiolitic rocks are tectonically emplaced on gneiss and schist forming a line with a NW–SE direction across the hydrological basin of the Anthemountas River (Fig. 1). In the Anthemountas basin, a variety of aquifers are developed such as porous, karst and fissured rock aquifers (Kazakis et al. 2013).

In the soils of the Anthemountas River basin, chromium (Cr) and manganese (Mn) are present. It has been already shown that these elements are of lithogenic origin, derived mainly from the weathering of ophiolitic rocks, that contain amphibole and pyroxene and/or clay minerals with ion substitution in the octahedral sites (serpentines) (Kazakis et al. 2015).

The first magnetic investigation of the soils in the study area was reported by Aidona et al. (2013). The authors presented the spatial distribution of the magnetic susceptibility in the broader area of the Anthemountas basin using

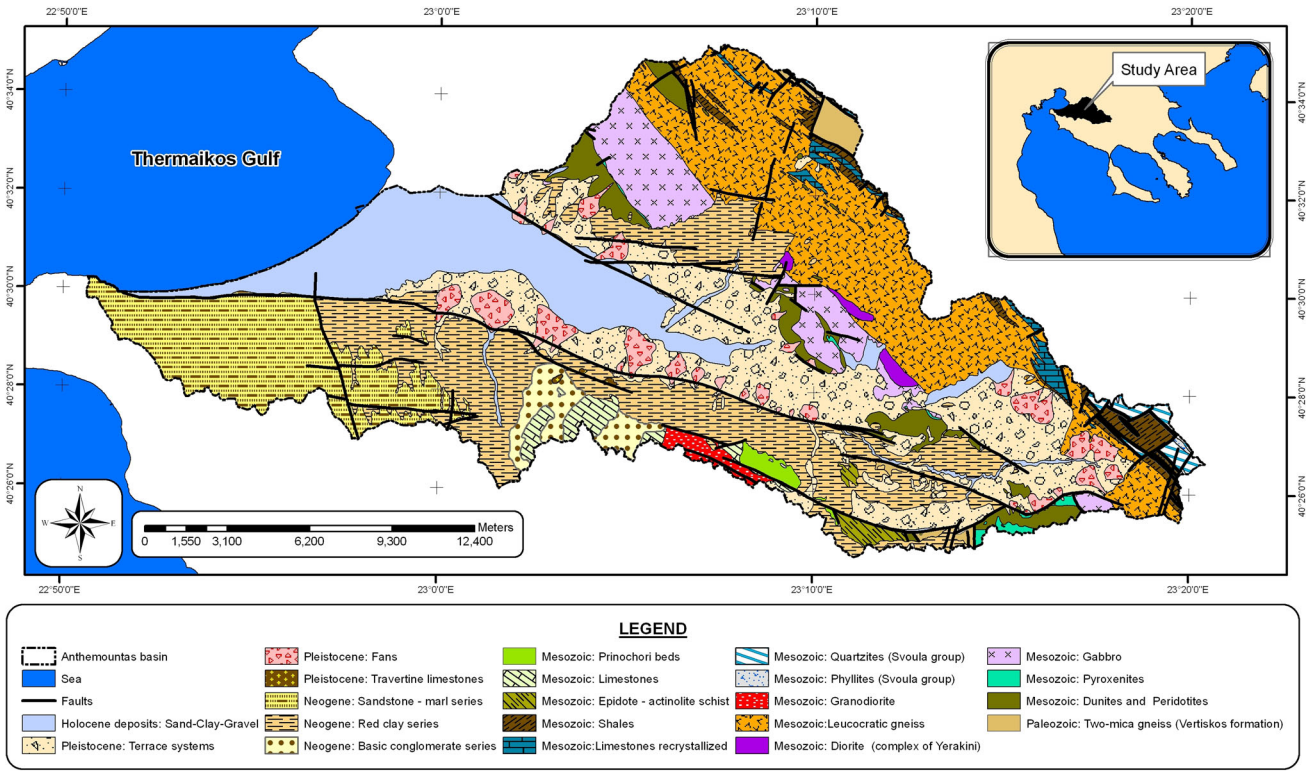

Fig. 1 Geological background of study area (from Aidona et al. 2013)

samples from 77 sites. The results revealed two areas with enhanced magnetic susceptibility values (Fig. 2): one along the northwest–southeast trending northern border of the basin with values of mass-specific magnetic susceptibility ranging from 80 to 423 $\times$ 10^{-8} m^3/kg and a second one in the basin's western most part, with medium to high values of mass-specific magnetic susceptibility ranging from 50 to 200 $\times$ 10^{-8} m^3/kg. According to the WRB (IUSS Working Group 2007), the investigated soils exhibit properties as anthrosols (as all the sampling areas consist of soils used mainly for agriculture). Soils indicate different soil textures in the two areas. In Area A, soils are more consistent, characterized as clay loam to sandy loam and originate from alluvial, marls, and clay sediments. On the contrary, in Area B the texture is more variable ranging from clay to sandy soils, because the soils originate from dunites, peridotites, and sediments of clay and terrace systems (Kazakis et al. 2014).

According to the last population census in 2011, around 80.000 residents live in the study area. However, the population density and the growth rate are dramatically changing. Area A hosts around 30,000 residents, and it shows the highest population increase over the last 30 years (776 %). In the Area B, there is only a small village with $\sim$2000 habitants and no significant population growth during the last decade was observed (22 %). Also the land use is different in the two areas. Area A is located in the vicinity of the International Airport of Thessaloniki City, a military base area, three big urban areas, and few arable fields. Area B is characterized by intense agricultural land use, and part of the area is covered by a forest.

Sampling and methodology

On the basis of the previous results, this study has focused in the two aforementioned areas (A and B) as presented in Fig. 2. From these two areas, soil samples from ten different sites have been selected (Fig. 3). At each sampling site, vertical hand core drilling was performed to maximum depth of 70 cm. The exact positions of sampling sites (recorded in WGS84 GPS coordinate system) are shown in (Fig. 2). The collected material of every 10 cm was homogenized and considered as one sample representative for this depth (e.g., sample E46-1 corresponds to profile number 46, composed from soil from the depth of 0–10 cm). The soil samples were dried and sieved through a 2-mm sieve and placed in plastic boxes of 2 $\times$ 2 $\times$ 2 cm. All samples derived from the first layer (0–10 cm) are considered as topsoils, while samples from the deepest layers in each profile (for the majority of the sites at the depth of 60–70 cm) are considered as subsoils. In order to enlarge the already existing surface magnetic susceptibility data in Area A, four additional transects were measured (Fig. 4) using the Bartington MS2D loop (Bartington Ltd., UK). For the first transect the average

measurement spacing was 100 m, while for the other three transects a mean step of 200 m was used. At each measuring point, up to 10 measurements were taken and a mean value was calculated.

Laboratory measurements of the volume-specific magnetic susceptibility (κ) have been taken with the Bartington MS2B dual-frequency sensor (Bartington Ltd., UK), using low and high frequencies 0.465 and 4.65 kHz (κ_{LF} and κ_{HF}), respectively. As the samples were weighed before the measurements, the results are expressed as mass-specific magnetic susceptibility (χ). Each sample was measured at least three times, and the values were averaged and corrected for the temperature drift of the pick-up coil. Frequency-dependent susceptibility (χ_{FD} %) was calculated according to Dearing et al. (1996) [χ_{FD} % = 100(χ_{LF} − - χ_{HF})/χ_{LF}]. According to Dearing's model (1996), a χ_{FD} % of 5 % or more indicates that the superparamagnetic (SP) particles are present in significant amounts.

Variation of the magnetic susceptibility (κ) with temperature (T °C) was measured using a KLY-4 Kappabridge with

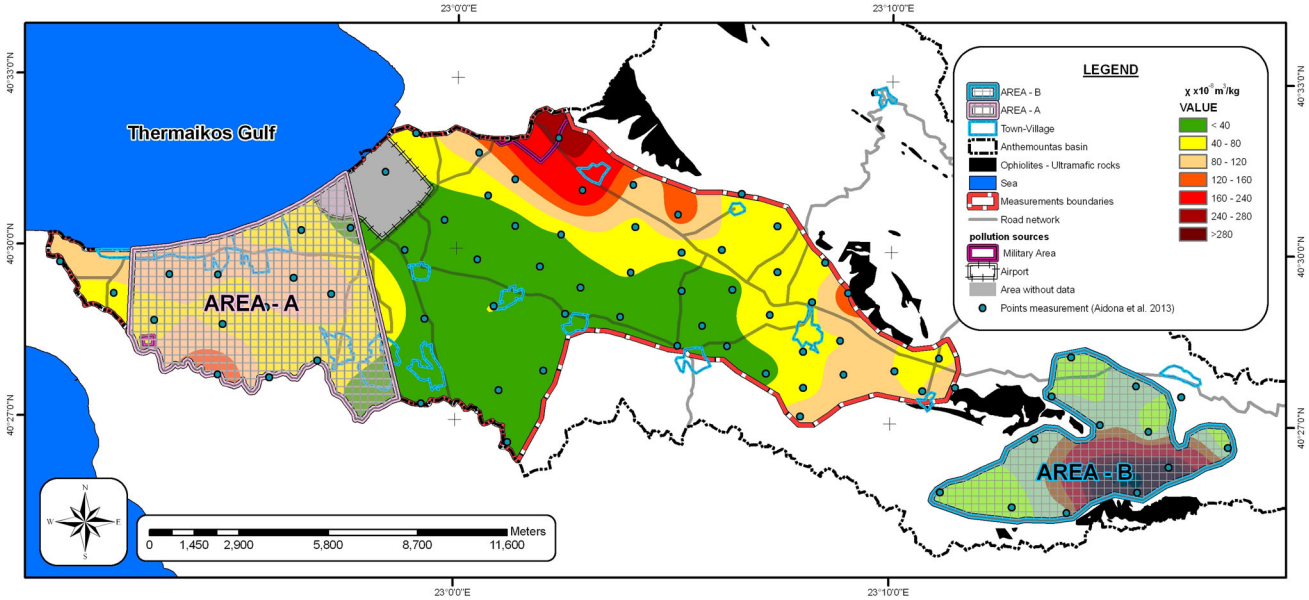

Fig. 2 Spatial distribution of mass-specific magnetic susceptibility (from Aidona et al. 2013). The two areas of the present study are highlighted with the *blue* and *red grids*

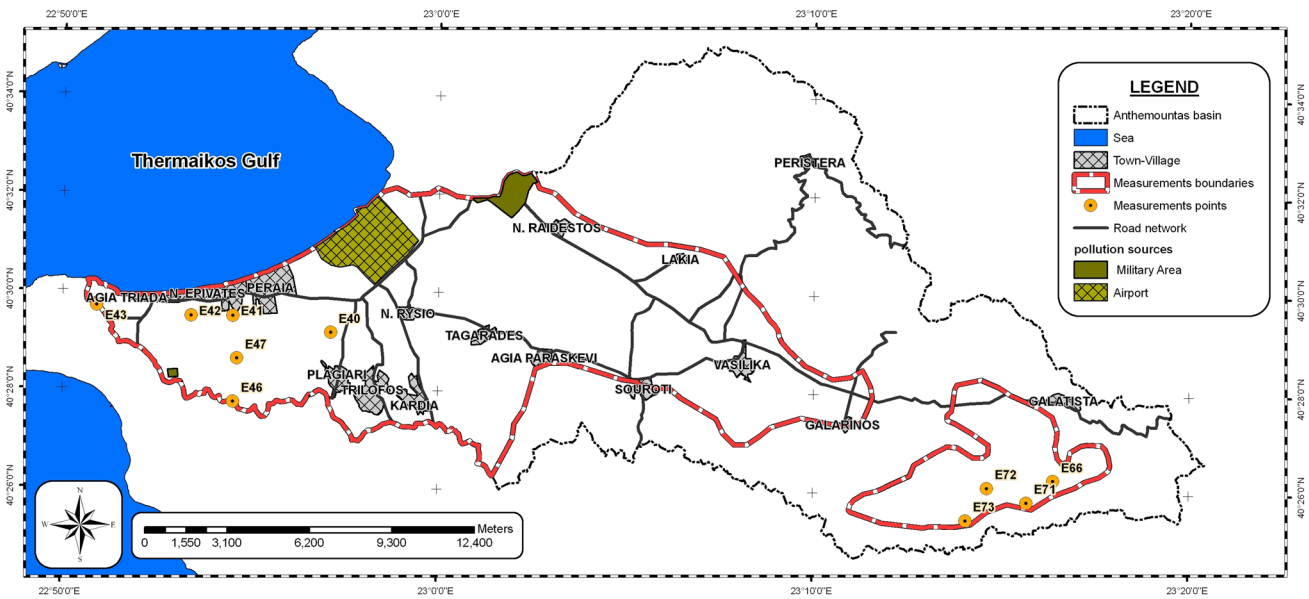

Fig. 3 Location of investigated soil profiles in the two areas

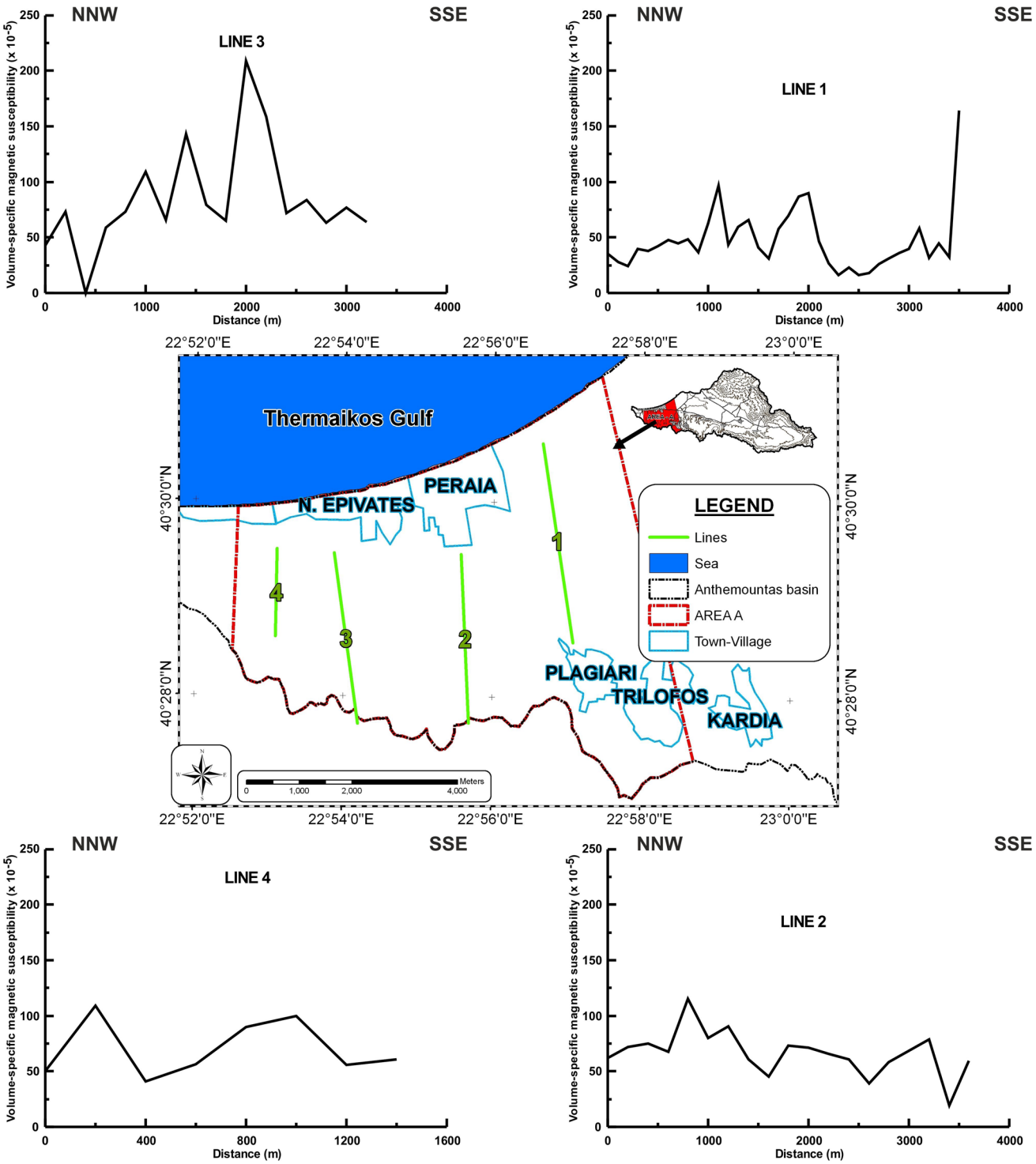

Fig. 4 Variation of volume-specific magnetic susceptibility measurements with distance performed on four transects in the Area A. All profiles are oriented from NNW to SSE

a CS-3 furnace (AGICO Ltd., Czech Republic). The main aim of these measurements was to compare the shape of obtained κ–T curves in topsoil and subsoil from both areas and to check possible changes in magnetomineralogy by determination of the characteristic temperatures of iron oxides (Curie/Néel/Verwey temperatures). The magnetomineralogy was determined by the Curie point estimation according to Petrovsky and Kapicka (2006) and Fabian et al. (2013).

Hysteresis loops and isothermal remanent magnetization (IRM) acquisitions were performed on selected topsoil and

subsoil samples from the two areas using a Princeton Sample Magnetometer VSM MicroMag 2900 (Princeton Measurements Corporation, USA) in order to assess the relative magnetic grain size (magnetic domain state), concentration of ferrimagnetic minerals, and their remanence characteristics. Magnetization and coercivity data [saturation magnetization (M_s), saturation remanence (M_{rs}), coercive force (B_c), and coercivity of remanence (B_{cr})] were displayed in the Day plot (e.g., Day et al. 1977; Dunlop 2002). IRM data were used to determine the S-ratio (ratio of remanent magnetization remaining after application of −300 mT following a previous saturation with a field of 1T). The S-ratio is sensitive to different contributions of magnetically 'soft' (magnetite, maghemite) and 'hard' (hematite, goethite) minerals (e.g., Thompson and Oldfield 1986). Curves of acquisition of remanence magnetization were numerically analyzed using the procedure described by Kruiver et al. (2001) in order to estimate the relative contribution of minerals with different magnetic hardness.

A Thermo Scientific X-ray fluorescence (XRF) analyzer Niton XL3t GOLD+ (Thermo Fisher Scientific Inc., USA) was used to determine the concentration of trace elements (Fe, Cr, Ni, Zn, Mn, Pb, and Ti). This instrument is designed to analyze groups of elements simultaneously in order to rapidly determine those elements present in the sample and their relative concentrations. In other words, the XRF peak height/intensity is generally indicative of its concentration (in mg/kg) and is achieved from fundamental parameter analysis (FP). FP analysis converts elemental peak intensities to elemental concentrations and/or film thicknesses. This is achieved typically though a calibration step, where the XRF response function (related to parameters that are independent of the sample matrix) for each element is measured using a known standard of some kind. The external calibration was not performed, because the aim of the present study is not to present absolute values, but to show general trend of the trace elements. Spectra were measured during an interval of 120 s, ensuring good quality of data with an average error of about ±0.7 %. Measurements were repeated several times (from 5 to 10) at different spots, and both weighted mean values as well as median values were calculated with their standard deviation. As a relatively small number of measurements were available for each sample (typically 7) and due to the occasional presence of outliers in these measurements that significantly affected the mean values, the median values were preferred as more representative. These median values were employed in all cases and used for all correlations with mass-specific magnetic susceptibility.

Representative samples from both areas were examined for morphology and elemental composition using a JEOL JSM-840A (JEOL USA, Inc., USA) Scanning electron microscope (SEM) equipped with an energy-dispersive X-ray spectrometer (EDS) INCA 300 (Oxford Instruments, UK) with 20 kV accelerating voltage and 0.4 mA probe current. Magnetic particles were separated from all samples using a hand magnet and were coated with carbon for SEM examination and EDS analyses.

The interpolation method of natural neighbor was used for the map of spatial distribution of the soil's magnetic properties using the Spatial Analyst Tools package. Therefore, raster files were produced with a cell size of 20 × 20 m and the values of each property were classified into six main classes. The final maps were created by overlaying the different thematic layers and are illustrated in the corresponding figures.

A cluster analysis has been employed as a simple approach of classifying samples into smaller coherent groups that can be correlated by location (Ledesma-Ruiz et al. 2015). The goal is that the samples within a group have to be similar to one another and different from (or unrelated to) the samples of other groups. There are numerous ways in which clusters can be formed. In this study, a hierarchical cluster analysis was performed. Hierarchical cluster analysis is an exploratory data analysis tool used to sort out different samples into groups (Danielsson et al. 1999). The levels of similarity at which samples are classified were used to construct the dendrogram (Chen et al. 2007). The Euclidean distance was used as a measure of similarity between every pair of samples (Hussein 2004). The distance between two samples (i and j) is given by:

$$d_{ij} = \left[\sum_{k=1}^{n} \left(X_{ik} - X_{jk}\right)^2\right]^{1/2}$$

where X_{ik} denotes the kth variable/parameter measured on sample i and X_{jk} is the kth variable measured on sample j.

Since the different parameters employ different units, standardized variables of the initial data were used with a mean value of 0 and a standard deviation of 1 (Voudouris et al. 1997). Furthermore, a K-means cluster algorithm analysis was applied to find the cluster centers of each property in each group. The K-means method is efficient in processing large datasets (Han and Kamber 2006). Goktepe et al. (2005) described in detail the mathematical background of the K-means algorithm.

Results

Magnetic properties

The distribution of the magnetic susceptibility values along the four examined transects are displayed in Fig. 4. The

volume-specific magnetic susceptibility values are ranging from 16 to 209 $\times 10^{-5}$, indicating magnetically enhanced topsoil signals. Line 1 shows the lower values of the four transects with a mean value of 47.1 $\times 10^{-5}$, while Lines 2 and 4 indicate more enhanced values of a mean value of 66.4 $\times 10^{-5}$ and 70.4 $\times 10^{-5}$, respectively. In all three transects, a smooth variation in the magnetic susceptibility values is observed indicating no large local magnetic anomalies. Line 3 reveals the highest values of volume-specific magnetic susceptibility (mean value 89.8 $\times 10^{-5}$) that gradually increased from 0 up to 2000 m. These detailed measurements are generally in good agreement with previous results reported in Aidona et al. (2013), presented in Fig. 2. A direct comparison between the two measuring methods cannot be performed since the initial results are expressed in mass-specific magnetic susceptibility values ($\times 10^{-8}$ m^3/kg), while the results along the examined transects are in volume-specific values ($\times 10^{-5}$). Studies by Kapicka et al. (1997, 2013) show that there is a significant correlation between surface κ measurements in situ and topsoil χ measurements in the laboratory. Therefore, the general trend showing higher values close to the Line 3 region (Fig. 2) is confirmed by this detailed magnetic susceptibility mapping of the area and is in agreement with the findings of Kapicka et al. (1997, 2013).

The calculated χ_{FD} % of top and subsoils from both areas are presented with corresponding low-field mass-specific magnetic susceptibility in Fig. 5. The majority of samples exhibits χ_{FD} % values <5 %, suggesting that the contribution of SP particles, as a result of pedogenic processes, can be considered as insignificant (Dearing 1994; Dearing et al. 1996). However, for samples 42-7, 43-1, 43-4, and 73-1, exhibiting χ_{FD} % >5 %, pedogenic influence should not be excluded.

The variation of the magnetic susceptibility with temperature is displayed in Fig. 6. Top and subsoil samples are examined from both areas (A, B). Investigated soils exhibit clear differences regarding the concentration of magnetic carriers between the two areas. In the case of Area A, a mixture of magnetite/maghemite with broad transition from ferri- to paramagnetic phase (520–590 °C) is prevalent, with obvious differences between the top and subsoil samples. On the other hand, top and subsoil samples from Area B indicate the presence of MD natural magnetite, with a narrow transition from 570 to 580 °C.

Magnetization and coercivity data (B_c, B_{cr}, M_s, M_{rs}) were measured for 23 top and subsoils samples from the two areas. The calculated ratios of B_{cr}/B_c and M_{rs}/M_s are displayed in the Day plot as modified by Dunlop (Dunlop 2002) in Fig. 7. The Day plot shows a clear differentiation in the investigated samples. In the Area A, topsoils show higher coercivity ratio (B_{cr}/B_c) than subsoil ones. A different distribution of values is observed in Area B. There is

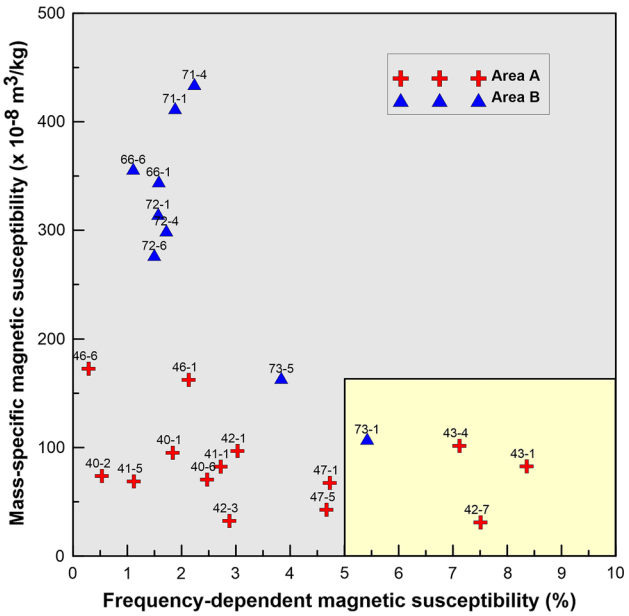

Fig. 5 Plot of mass-specific magnetic susceptibility versus frequency-dependent magnetic susceptibility of soil samples composed for the two studied areas

no discrimination between top and subsoil samples; all the examined samples form a single cluster independent from their depths. Nevertheless, Area B is clearly separated from the two groups of the top and subsoils of Area A, which indicates a dominant lithological influence in this area. All magnetic properties are presented in Table 1.

IRM acquisition curves show that in all cases a low-coercivity magnetic phase like magnetite is dominant since the saturation of IRM is achieved in low fields (~0.3 T). The decomposition of IRM into different coercivity components was performed using the procedure described by Kruiver et al. (2001). On average, the first component does not show a difference between the two areas, whereas the second component differs. Area A contains increased content of high-coercivity minerals (magnetically 'hard'), which is in agreement with the results of the S-ratio. These findings are not in agreement with the Day plot, which is based on integrated data. However, there is no systematic discrimination between samples from different soil layers. This can be explained by the presence of variable magnetic mineralogy, composed of material with different magnetic phases. It seems that in the present study the IRM decomposition can be used as a diagnostic tool for discrimination between the two regions, but not between different soil layers (top vs. subsoil). Corresponding data of IRM coercivity components are shown in Table 2.

Remanence characteristics represented by the S-ratio are presented in Fig. 8. All samples from Area B show S-ratio values near 1, reflecting the dominance of ferrimagnetic minerals (magnetite and/or maghemite) independent of

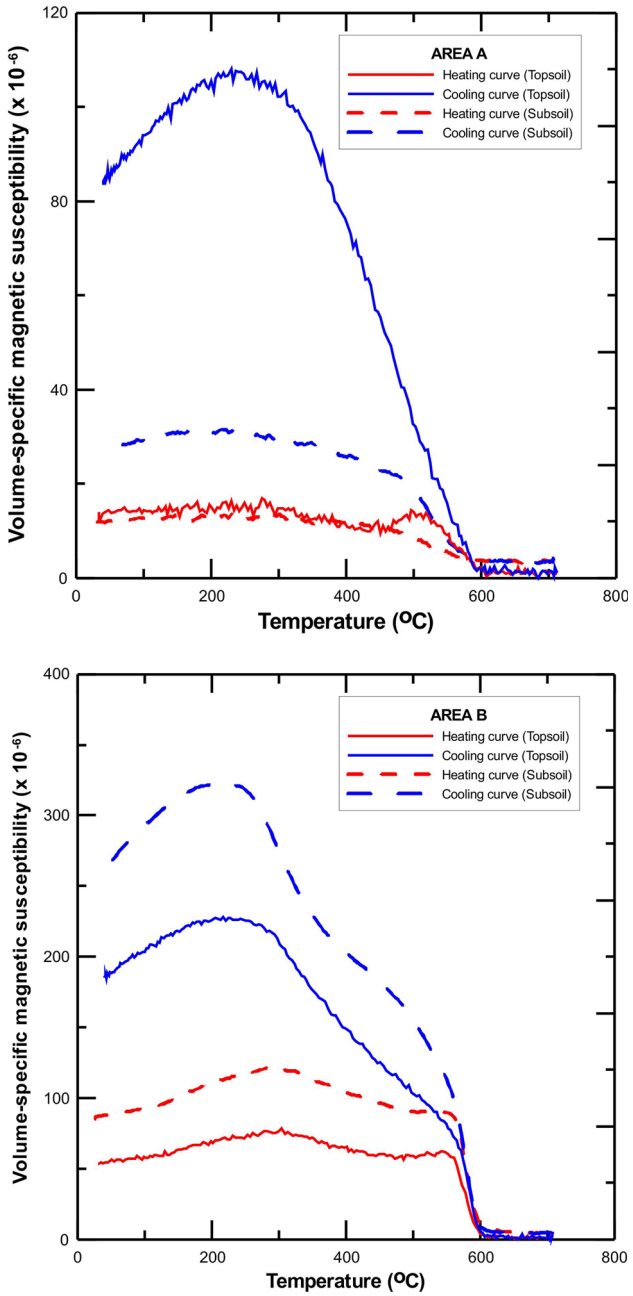

Fig. 6 Volume-specific magnetic susceptibility versus temperature. Thermomagnetic curves of soil samples from Area A: 42-1 (topsoil), 42-6 (subsoil) and soil samples from Area B: 72-1 (topsoil), 72-6 (subsoil)

grain size. High magnetic susceptibility of all samples also reveals increased amount of ferrimagnetic minerals. On the other hand, soils in Area A show smaller mass-specific magnetic susceptibility than in Area B, with more scattered S-ratio values between 0.85 and 0.95. This pattern suggests an increased concentration of magnetic minerals with higher coercivity remanence, most probably antiferromagnetic hematite or highly heterogeneous magnetite with

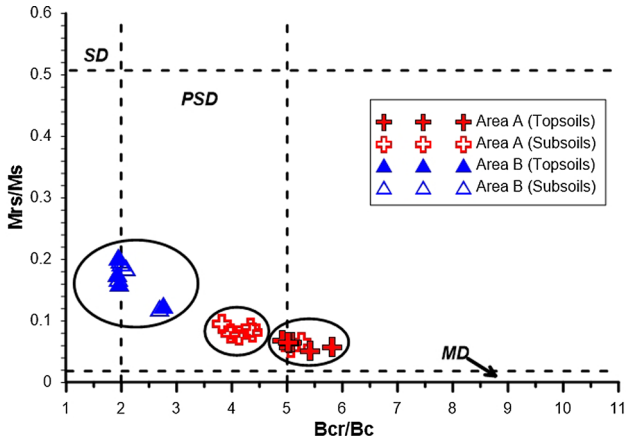

Fig. 7 Day plot compares top and subsoil samples composed for the two studied areas

many structural defects. The later mineral may come from industrial sources.

Trace elements

The trace elements analyses were performed on enlarged sets of topsoil samples from the two areas (in total 26 sites, 13 from each area).

Figure 9 shows the correlations between mass-specific magnetic susceptibility and relative concentration of trace elements (Fe, Cr, Ni, Mn, Zn, Pb, and Ti) separately for the two areas (expressed in mg/kg). In cases of the Fe, Ti, Pb, Cr, Ni, and Mn, the distinction of the two areas is significant. Higher concentration of the Fe, Cr, Ni, and Mn in Area B than in Area A can be associated with the ophiolitic parent rocks and their products. On the contrary, increased concentrations of Pb and Ti are found in Area A. Strong and moderate correlations between magnetic susceptibility and concentrations of Cr and Pb, respectively, may be attributed to the anthropogenic origin of these elements. Summary statistics of the studied elements, separately for the two areas, are displayed in Table 3.

Morphological and elemental composition of magnetic particles

A detailed morphological and elemental composition of magnetic particles can allow their correlation to anthropogenic sources or traffic activities (Adachi and Tainosho 2004). Morphological characterization of magnetic particles from Area A reveals significant differences between top and subsoil. Topsoil magnetic particles appear near-spherical, angular, or flake-like (Fig. 10a–c). Near-spherical particles (Fig. 10a) are Fe rich (>70 wt%) with variable amounts of Ti and Mn (up to 5.5 wt% and <1.0 wt%, respectively) and are considered to have derived from

Table 1 Main magnetic properties of studied soil samples

Sample	B_{cr} (mT)	B_c (mT)	M_s (Am^2/kg)	M_{rs} (Am^2/kg)	B_{cr}/B_c	M_{rs}/M_s	χ ($10^{-8}m^3/kg$)	χ_{FD} %
40-1	29.36	5.41	0.137	0.007	5.42	0.05	97.6	1.84
40-2	32.65	5.62	0.096	0.006	5.81	0.06	76.0	0.53
40-6	30.11	7.29	0.111	0.008	4.13	0.08	72.8	2.47
41-1	32.66	6.51	0.101	0.007	5.02	0.07	84.6	2.72
41-5	29.59	7.44	0.099	0.008	3.98	0.08	71.2	1.12
42-1	31.66	6.30	0.124	0.008	5.03	0.06	99.1	3.03
42-3	38.71	8.92	0.043	0.004	4.34	0.09	34.7	2.88
42-7	27.25	7.14	0.026	0.002	3.82	0.09	33.3	7.51
43-1	32.15	6.32	0.091	0.006	5.08	0.07	84.9	8.36
43-4	32.78	7.49	0.078	0.006	4.38	0.08	103.9	7.12
46-1	34.49	6.83	0.217	0.014	5.05	0.07	164.7	2.13
46-6	27.63	5.45	0.238	0.013	5.07	0.06	175.0	0.29
47-1	36.39	7.40	0.084	0.006	4.92	0.07	69.7	4.73
47-5	27.47	14.21	0.018	0.001	5.25	0.06	45.0	4.67
66-1	25.79	13.22	0.504	0.089	1.93	0.18	347.5	1.58
66-6	34.69	17.85	0.514	0.088	1.95	0.17	359.0	1.11
71-1	34.41	17.37	0.610	0.125	1.94	0.20	415.1	1.88
71-4	31.38	15.94	0.274	0.055	1.98	0.20	437.2	2.24
72-1	31.38	15.70	0.587	0.095	1.97	0.16	317.6	1.57
72-4	33.53	16.11	0.450	0.088	2.00	0.19	302.2	1.72
72-6	25.54	9.26	0.422	0.079	2.08	0.19	279.6	1.50
73-1	23.75	8.82	0.105	0.013	2.76	0.13	110.6	5.42
73-5	29.36	5.41	0.140	0.017	2.69	0.12	166.6	3.84

B_{cr}, coercivity of remanence; B_c, coercive force; M_s, saturation magnetization; M_{rs}, saturation remanence; B_{cr}/B_c, coercivity ratio; M_{rs}/M_s, magnetization ratio; χ, mass-specific magnetic susceptibility; χ_{FD} %, percentage of frequency-dependent magnetic susceptibility

industrial activities (Magiera et al. 2008) and domestic heating systems (Tissari et al. 2008). Non-spherical particles contain Fe (>75 wt%), Ti (up to 6.5 wt%), Mn (up to 2 wt%) and minor amounts of Cr, Ni, and Cu (all below 1 wt%). The presence of Cu and Cr supports the origin of these particles from brake and wear materials (Thorpe and Harrison 2008; Chaparro et al. 2010; Pachauri et al. 2013). Their morphological characteristics suggest that they have been released from vehicles via exhaust emission and from the abrasion or corrosion of the vehicle engine and body work (Thorpe and Harrison 2008; Pachauri et al. 2013). Pb is below detection limits in all cases. Conversely, the majority of magnetic particles from the subsoil of Area A have a different morphology. They appear as crystals of Fe-oxide minerals, pointing to their formation by natural processes (Fig. 10d).

The largest fraction of magnetic particles from top and subsoil of Area B shows similar morphology and elemental composition. The particles appear crystal shaped and rounded at the edges, suggesting that they have derived from rock erosion of the surrounding area (Fig. 10e, f). Crystals with profound crystallographic geometry can result from natural processes (e.g., magma crystallization) which allowed all crystal faces to develop. Crystals are recognized as magnetite (Fe oxide) and chromite (Fe–Cr oxide) with minor amounts of Ti and Mn elements that occur in the crystal lattice of both minerals. The same minerals are also identified in the subsoil of Area A. These minerals are constituents of the rocks that are found in the investigated area.

Cluster analysis

The output of a cluster analysis is a dendrogram (or tree diagram) connecting the samples with the large similarities. The results of the cluster analysis show that the examined samples can be grouped into distinctive clusters, according to the dendrogram shown in Fig. 11. The dendrogram rendered 23 soil samples into two statistically significant groups (clusters) with similar magnetic properties. Table 4 shows the final cluster centers for each variable in each soil group. As can be observed, the data are classified into two dominant groups, corresponding to each area (A and B). All the samples collected from the Area A are found to be in cluster 1, while the majority of samples from the Area B are found to be in cluster 2.

Table 2 Coercivity components in all studied samples analyzed according to Kruiver et al. (2001)

Sample	First component			Second component		
	(%)	$B_{1/2}$ (mT)	DP	(%)	$B_{1/2}$ (mT)	DP
40-1	86	39.8	0.29	14	316.2	0.33
40-2	80	39.8	0.30	20	199.5	0.40
40-6	86	39.8	0.28	14	199.5	0.30
41-1	89	39.8	0.28	11	199.5	0.28
41-5	91	38.0	0.27	9	199.5	0.13
42-1	97	42.6	0.35	3	199.5	0.20
42-3	97	50.1	0.37	3	501.1	0.10
42-7	97	39.8	0.35	3	501.1	0.08
43-1	83	37.1	0.25	17	177.8	0.20
43-4	94	42.6	0.33	6	338.8	0.20
46-1	98	47.8	0.35	2	630.9	0.20
46-6	89	36.3	0.30	11	398.1	0.60
47-1	90	45.7	0.33	10	316.2	0.20
47-5	89	46.7	0.33	11	316.2	0.15
66-1	97	39.8	0.26	3	251.2	0.18
66-6	100	39.8	0.30	–	–	–
71-1	98	47.8	0.26	2	199.5	0.10
71-4	78	39.8	0.22	22	100.0	0.20
72-1	95	44.6	0.27	5	199.5	0.22
72-4	93	42.6	0.27	8	158.5	0.20
72-6	98	44.6	0.30	2	501.1	0.08
73-1	97	39.3	0.30	3	316.2	0.20
73-5	96	37.1	0.27	4	251.2	0.20

(%), the percentage of the coercivity components; $B_{1/2}$, the mean coercivity corresponds to the applied field at which the mineral phase would acquire half of its saturation IRM; *DP*, the dispersion parameter expressing the coercivity distribution of the mineral component and corresponding to one standard deviation of the lognormal function

Discussion

It is well known that the enhancement of the magnetic susceptibility in the topsoils is associated with heavy metal concentration; therefore, it can be considered as a first indicator of soil contamination.

The most common approach, to detect anthropogenic anomalies, is the calculation of the difference between top and subsoil. It is reported in Hanesch and Scholger (2002) that high values of magnetic susceptibility in the uppermost 20 cm of the soil reflect an anthropogenic influence, while lower values indicate the dominance of lithological influence. If this difference is more than 20×10^{-8} m^3/kg, then an anthropogenic anomaly is identified. On the contrary, when the difference is below -20×10^{-8} m^3/kg, the anomaly is controlled by lithology. The vertical distribution of magnetic susceptibility has been also studied by other authors leading to the similar conclusions. Maher

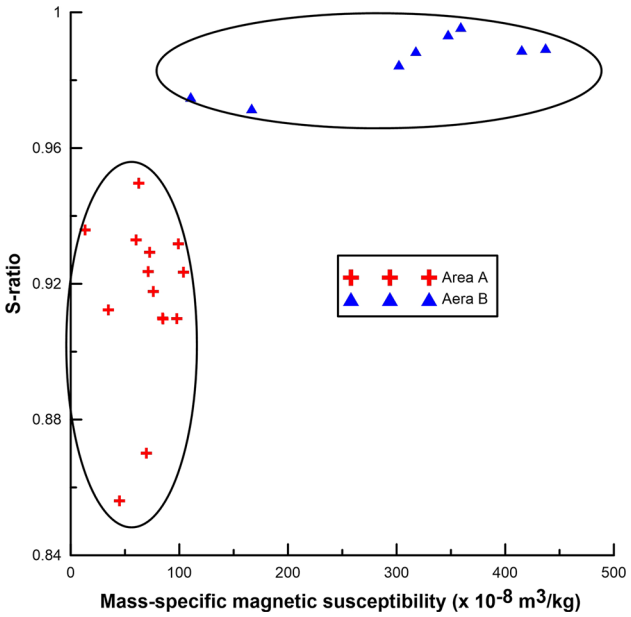

Fig. 8 Correlation between S-ratio and mass-specific magnetic susceptibility of soil samples composed for the two studied areas

(1986) investigated several types of soils in order to characterize them on the basis of the magnetic mineral measurements. Examples of soils developed from doleritic parent rock showed a steady increase of χ with depth. Furthermore, soils that have been affected from atmospheric pollution showed the reverse behavior; i.e., decreased values of χ with depth. Similar results concerning the variation of χ in vertical soils profiles from China have been reported by Lu and Bai (2006). Magiera et al. (2006) attempted to discriminate the lithogenic and anthropogenic influence on topsoil using magnetic susceptibility measurements. Their study of the vertical profiles showed again increased χ values in the forest topsoils and, in the polluted areas, decreased χ values in subsoils. Apart from the vertical distribution of magnetic susceptibility, Hanesch and Scholger (2005) studied the influence of the soil type on the magnetic susceptibility through profiles concluding that the differences of the topsoil in relation to the subsoil depend more on the lithology than on the soil type. However, the vertical profiles of magnetic susceptibility in both areas did not show a similar distribution as described by the previous authors and they did not follow the threshold suggested by Hanesch and Scholger (2002). This pattern was one of our main motivations for extending the investigation in this area by studying additionally magnetic properties.

There is no systematic increase in frequency-dependent magnetic susceptibility over the whole study area. Increased values were only observed occasionally, in a few distinct samples. Therefore, this observation is not interpreted as the result of general pedogenesis. The volume-

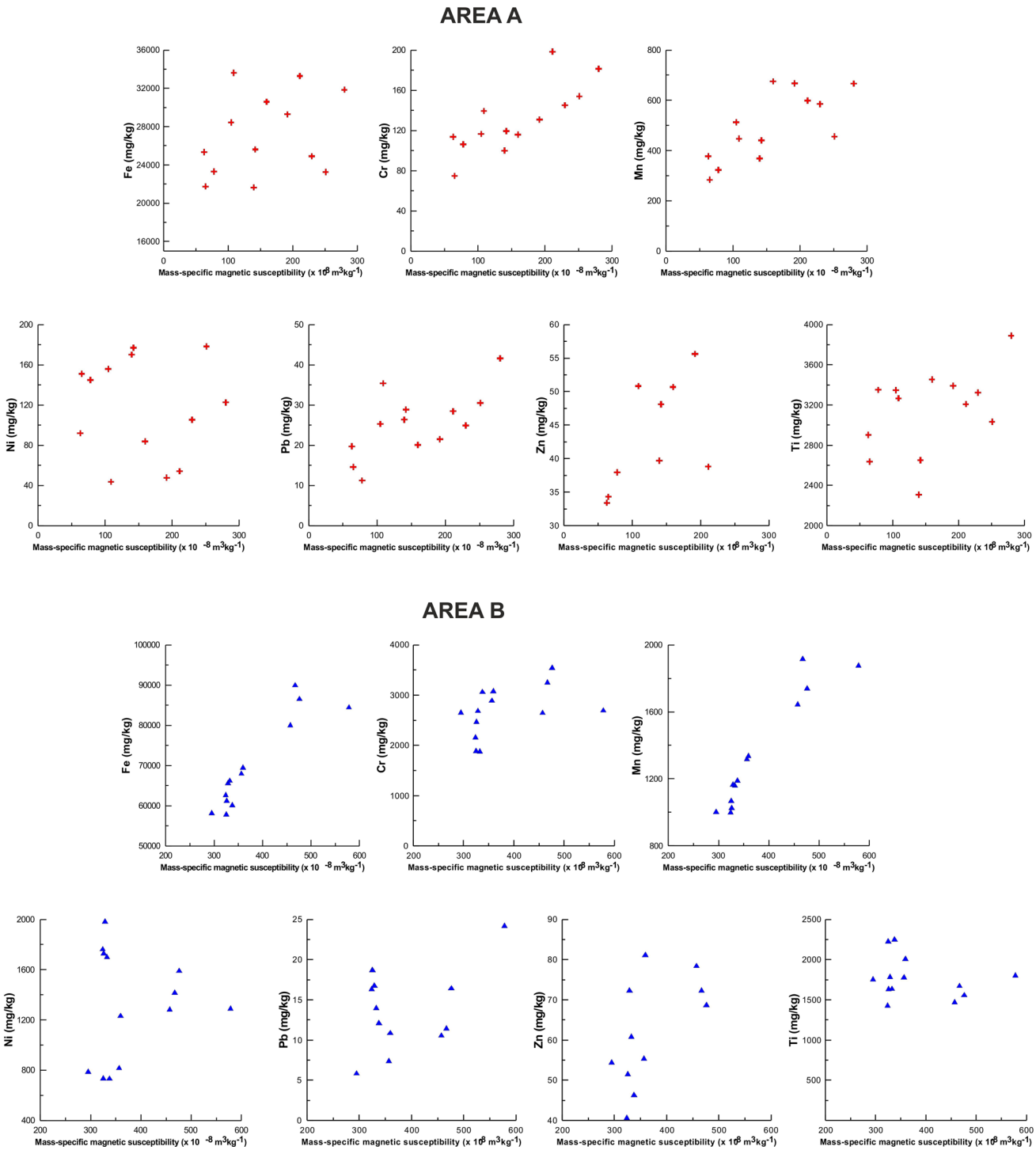

Fig. 9 Correlation between mass-specific magnetic susceptibility and concentration of trace elements for the two studied areas separately

specific susceptibility values are rather high (present range). Therefore, the increased frequency-dependent values cannot be attributed to rounding error due to low sensitivity of the Bartington instrument. Hence local effects should be considered as more plausible. For example, different land use in the past (plugging, fertilization, etc.) might cause buried soil layers with a higher portion of ultrafine iron oxides. Local anomalies in the soil properties could be also caused by different vegetation cover in the past. The other possible source may be linked to local floods. However, to the best of our knowledge, this area has been not flooded. Finally, local depressions in the

Table 3 Summary statistics of the major trace elements concentrations (in mg/kg) for the two areas

Element	*N*	Mean	Median	Min	Max	SD	Skewness
Area A							
Fe	13	27,260.2	25,733.6	21,762.1	33,724.5	4280	0.25
Cr	13	130.5	119.4	74.8	198.4	33.5	0.62
Mn	13	492.8	456.3	286.9	675.8	135.9	0.04
Ni	13	117.4	122.7	43.6	178.3	49.7	−0.28
Pb	13	52.4	46.9	33.5	112.2	24.3	1.87
Zn	13	25.2	25.3	11.2	41.6	8.2	0.23
Ti	13	3146.5	3278.4	2317.9	3899.5	420.0	−0.42
Area B							
Fe	13	70,194.1	66,402.5	57,952.5	90,140.5	11,326.8	0.73
Cr	13	2720.3	2722.2	1913.2	3578.4	500.3	−0.19
Mn	13	1346.3	1193.0	1004.1	1921.1	336.8	0.74
Ni	13	1318.0	1296.7	738.4	1987.4	434.4	−0.13
Pb	13	14.3	14.2	6.1	24.4	5.1	0.23
Zn	13	61.8	58.5	41.1	81.5	12.9	0.07
Ti	13	1792.4	1779.0	1450.1	2270.6	256.9	0.79

N number of samples, *SD* standard deviation

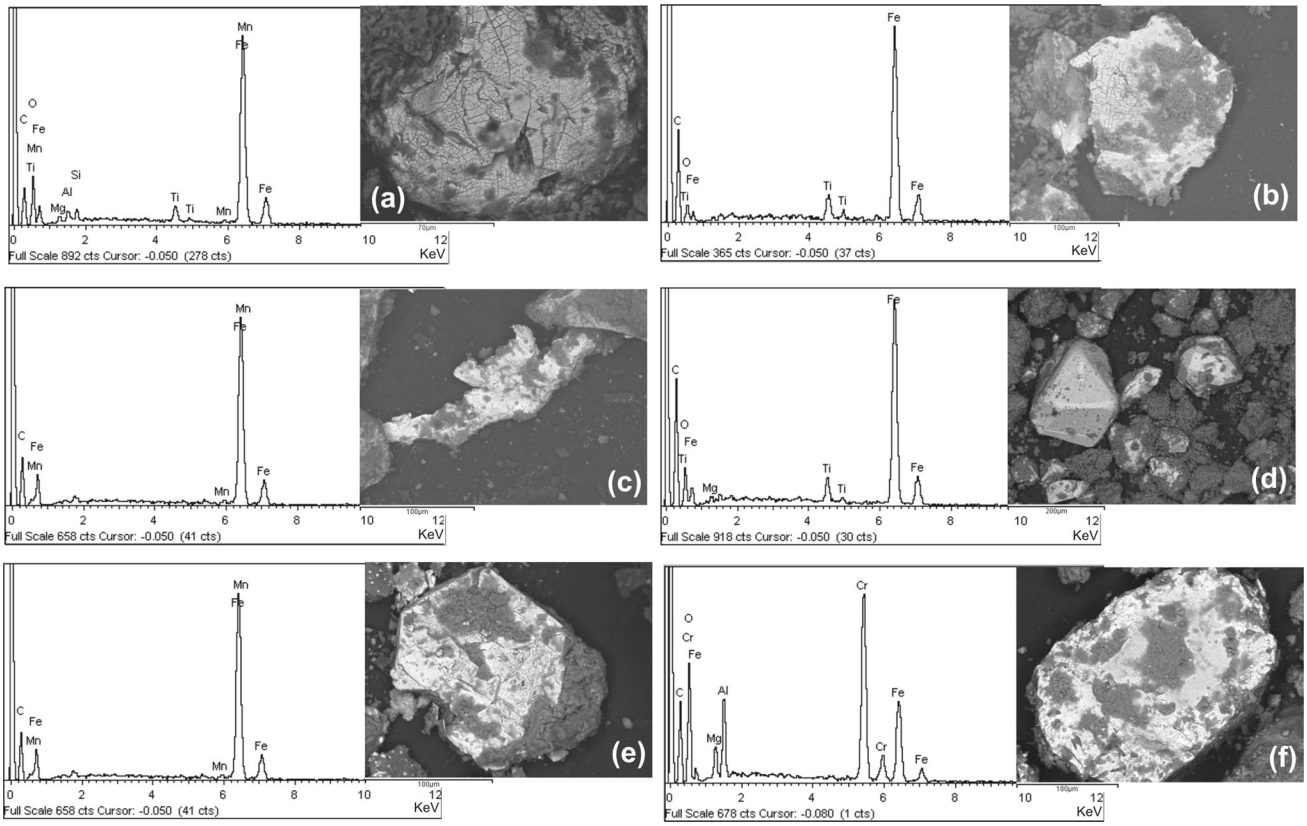

Fig. 10 SEM images in back-scattered electrons mode and EDS spectrum of specified spots of magnetic particles separated from Area A topsoil (**a–c**) and subsoil (**d**) and from Area B topsoil (**e**) and subsoil (**f**)

impermeable solid geological basement may cause increased humidity of the soil layer, which may result in local pedogenesis and formation of ultrafine iron oxides (Torrent et al. 2010). Although this observation is not so important for the purpose of this paper, the above effects should be studied in more detail.

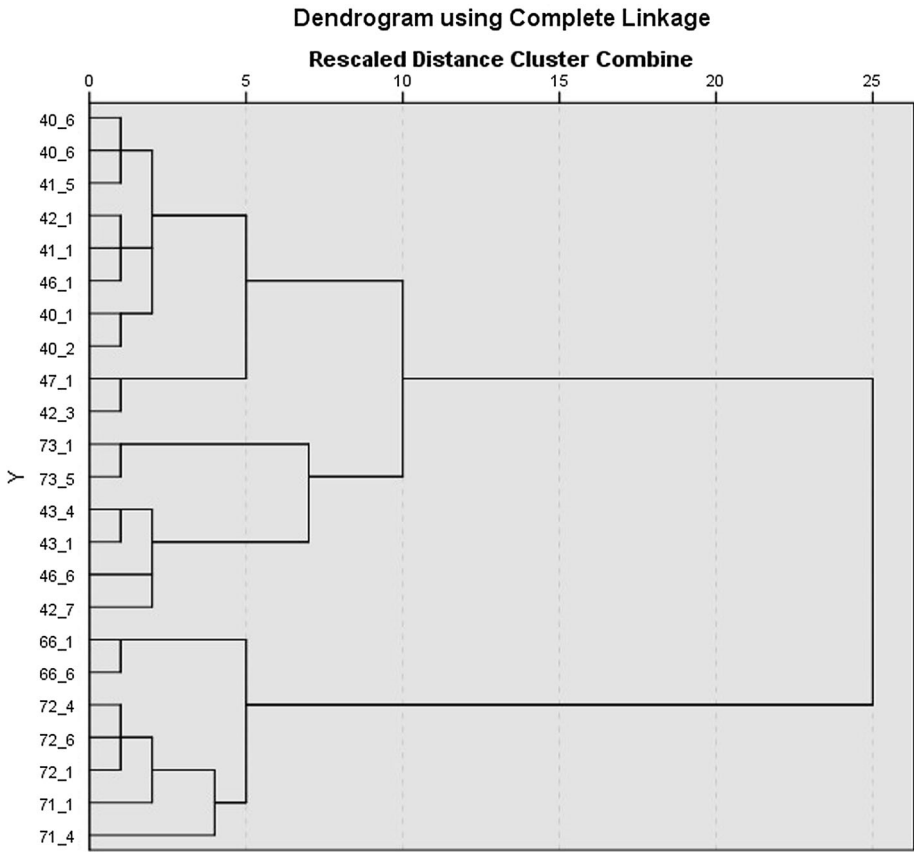

Fig. 11 Dendrogram defining two soil groups based on hierarchical cluster analysis

Table 4 Results of cluster analysis: Cluster centers of each property in two groups

Parameter	Cluster centers	
	1	2
B_{cr} (mT)	31.230	30.920
B_c (mT)	15.770	7.092
M_{rs} (Am^2/kg)	0.480	0.112
M_r (Am^2/kg)	0.088	0.008
B_{cr}/B_c	1.979	4.476
M_{rs}/M_s	0.185	0.078
χ ($10^{-8}m^3/kg$)	351.120	81.230
χ_{FD} %	1.657	4.061

The present study has mainly attempted to define the different contributions to the magnetic susceptibility values in the investigated areas. The preliminary results from the spatial distribution of susceptibility (Aidona et al. 2013 Fig. 2) lead us to the conclusion that Area A reflects the anthropogenic influence due to its vicinity to the urban area and the airport of Thessaloniki. On the other hand, Area B, close to the ophiolitic basement, showed a more complex situation since higher values of magnetic susceptibility are found along the whole length of studied profiles (up to 70 cm depth). Thus, the authors considered that Area B may be affected from both anthropogenic (in topsoil) and lithogenic particle contributions.

The results of the present study clearly show that in Area A the magnetic susceptibility values are primarily enhanced due to anthropogenic anomalies and confirm the earlier conclusions of Aidona et al. (2013). The magnetic properties of topsoils are different than the subsoils. The above result is in a good agreement with the results of Fialova et al. (2006) who studied the magnetic properties of soils in polluted areas, showing that the anthropogenic contribution can be clearly recognized and discriminated from the lithogenic ones in an area where lithology is poor in Fe oxides. In the case of study of Fialova et al. (2006), the Day plot did not show clear discrimination between lithogenic and anthropogenic contributions. However, in the present study, the Day plot (Fig. 7) easily distinguishes soils from Area B and top and subsoils from the Area A. In Area A, the topsoils span over the transition zone from pseudo-single domain to multidomain magnetic grain size, while the subsoils seem to be dominated by multidomain grains. On the contrary, the magnetic properties in Area B indicate that there is no discrimination between top and subsoil; soils exhibit a low coercivity ratio (B_{cr}/B_c) with a high magnetization ratio (M_{rs}/M_s).

The geochemical analysis shows that in Area A, the anthropogenic sources mainly contribute the elements of

Pb as indicated by the XRF analyses. The soil analysis of Pb shows concentrations in Area A of about 30 mg/kg, while in Area B the mean values of Pb are up to 17 mg/kg. According to Rudnick and Gao (2003), the lithogenic concentration of Pb in the earth's crust is 17 mg/kg. The above estimation confirms our result that Pb concentrations in Area A may be associated with anthropogenic sources. The presence of trace elements such as Pb, Cr, and Zn in polluted areas has been reported in several other studies (e.g., Hanesch and Scholger 2002; Lu and Bai 2006; Bourliva et al. 2011; Jordanova et al. 2014). Significant correlation between Cr and magnetic susceptibility shows that even low concentrations of Cr may reflect influence of industrial activities. The soil pollution highlights the necessity of a more detailed research of the geochemical composition of the soils at greater depths. Moreover, the research could also be extended to monitoring of the contamination of groundwater by Pb as in this part of the Anthemountas basin the groundwater is characterized by very high pollution risk from the superficial activities (Kazakis and Voudouris 2015). Despite the fact that a less reliable correlation is found between magnetic susceptibility and concentration of Pb, this can be used as a first-level proxy for determination of this trace element. On the other hand, Zn, which is usually associated with polluted areas, does not show any significant enhancement in Area A compared to other urban soils and shows only a weak correlation with magnetic susceptibility. This unexpected distribution in combination with the relative moderate concentrations of Pb may be related to the soil texture in this region. The sandy soils in this area are probably not able to accumulate the trace elements in the topsoil (upper 10 cm), highlighting the importance of the soil texture. However, more detailed sampling and analysis along vertical profiles are needed in order to confirm the above estimation.

The magnetic susceptibility in Area B is strongly related to the products of the ophiolitic rock's weathering and their escalated concentration of Cr and Mn. The geochemical composition of the soil samples is in accordance with the previous study of Kazakis et al. (2015), where the authors showed that Cr and Mn in the Anthemountas basin originate from the mafic minerals. According to the above results, for Area B there is only a lithogenic influence in the soils and the preliminary hypothesis set by Aidona et al. (2013)—that both influences are affecting the soils—cannot be confirmed.

In summary, the results of the present study confirm that the magnetic properties of soils can be used to determine the origin of the pollution in a region. Large-scale measurements of magnetic properties as a first step should be followed by a final detailed and integrated investigation. The areas suspected to have anthropogenic pollution can be spatially constrained by the first step, whereas detailed and integrated measurements can confirm or not the origin of the pollutants. However, before any further interpretation, a particular caution has to be taken when a magnetically enhanced geological background is dominant in the investigated area.

Conclusions

The results of the present study reveal that investigated soils from two areas in Anthemountas River basin differ regarding their magnetic properties. Area A seems to be affected by anthropogenic activity (mainly traffic and local heating), while Area B is influenced by a highly magnetic geological background (ophiolitic parent material). Magnetic discrimination between the two areas is efficiently shown by a Day plot, based on the magnetization and coercivity ratios. The remanence characteristics expressed by the S-ratio also efficiently discriminates the investigated samples, suggesting antiferromagnetic minerals in soils from Area A. In Area B, only ferrimagnetic minerals, such as magnetite/maghemite, seem to be present. Variations in magnetic susceptibility with temperature confirmed the above results.

Magnetic enhancement in Area A seems to be associated with a magnetic fraction accompanying Pb emission sources indicating the degree of contribution of anthropogenic sources. A significant correlation between mass-specific magnetic susceptibility and concentrations of Cr, Mn, and Pb in Area A is observed. In Area B, concentrations of Fe, Ni, and Mn are associated with mass-specific magnetic susceptibility. Strong and moderate correlations with Cr and Pb, respectively, in Area A may indicate topsoil pollution caused by industrial activities. An increased concentration of Cr and Mn in Area B is related to weathering products of the ophiolitic parent material basement.

Scanning electron microscopy with energy-dispersive spectrometric analyses was performed on selected samples and show a similar differentiation between the two areas.

These results are confirmed by the cluster analysis from which two main groups of soil samples have been identified, essentially corresponding to the two examined areas (A and B).

Magnetic properties have proved to be successful in the discrimination of different sources responsible for the enhancement of magnetic susceptibility. One has to keep in mind that high magnetic susceptibility of topsoils is not necessarily associated with dominant anthropogenic input and background geology should be always taken into consideration. Consequently, anthropogenic magnetic signals may be masked by high values of magnetic

susceptibility of lithogenic origin. Therefore, a detailed study of different contributions is needed.

Acknowledgments This study was partly supported by the bilateral educational program between Greece and Czech Republic and by the Czech Science Foundation Grant No. 13-10775S. Eduard Petrovsky is grateful for the support provided by the Ministry of Education, Youth and Sports of the Czech Republic through INGO Project LG15036. Authors would like to thank the three anonymous reviewers and the editor for their constructive comments that significantly helped to improve this paper.

References

Adachi K, Tainosho Y (2004) Characterization of heavy metal particles embedded in tire dust. Environ Int 30:1009–1017

Aidona E, Kazakis N, Mavroidaki K, Voudouris K (2013) Magnetic susceptibility as a tool for the discrimination of anthropogenic and lithogenic history of topsoils: preliminary results from the broader area of Thessaloniki city. Bull Geol Soc Greece XLVII:236–244

Botsou F, Karageorgis AP, Dassenakis E, Scoullos M (2011) Assessment of heavy metal contamination and mineral magnetic characterization of the Asopos River sediments (Central Greece). Mar Poll Bull 62:547–563

Bourliva A, Kantiranis N, Papadopoulou L, Aidona E, Christoforidis G, Kollias P (2011) On the morphology, geochemical characteristics and magnetic properties of urban road dust particles from the historic center of the city of Thessaloniki, Greece. In: Proceedings of the 12th international conference on environment science and technology, Rhodes, Greece, 8–10 Sep 2011

Boyko T, Scholger R, Stanjek H (2004) Topsoil magnetic susceptibility mapping as a tool for pollution monitoring: repeatability of in situ measurements. J Appl Geophys 55:249–259

Chaparro MAE, Marie DC, Gogorza CSG, Navas A, Sinito AM (2010) Magnetic studies and scanning electron microscopy-X-ray energy dispersive spectroscopy analyses of road sediments, soils and vehicle-derived emissions. Stud Geophys Geod 54:633–650

Chen K, Jiao JJ, Huang J, Huang R (2007) Multivariate statistical evaluation of trace elements in groundwater in a coastal area in Shenzhen, China. Environ Poll 147(3):771–780

Danielsson A, Cato I, Carman R, Rahm L (1999) Spatial clustering of metals in the sediments of the Skagerrak/Kattegat. Appl Geochem 14:689–706

Day R, Fuller MD, Schmidt VA (1977) Hysteresis parameters of titanomagnetites: grain size and composition dependence. Phys Earth Planet Int 13:260–267

Dearing JA (1994) Environmental magnetic susceptibility: using the Barrington MS2 system. Chi Publishing, Kenilworth

Dearing JA, Dann RJL, Hay K, Lees JA, Loveland PJ, Maher BA, O'grady K (1996) Frequency-dependent susceptibility measurements of environmental materials. Geophys J Int 124:228–240. doi:10.1111/j.1365-246X.1996.tb06366.x

Dikau R (1989) The application of a digital relief model to landform analysis. In: Raper JF (ed) Three dimensional applications in geographical information systems. Taylor and Francis, London, pp 51–77

Dunlop DJ (2002) Theory and application of the day plot (M_{rs}/M_s vs H_{cr}/H_c): application to data for rocks, sediments and soils. J Geophys Res 107:1–15

Fabian K, Shcherbakov VP, McEnroe SA (2013) Measuring the Curie temperature. Geochem Geophys Geosyst 14:947–961

Fialova H, Maier G, Petrovsky E, Kapicka A, Boyko T, Scholger R (2006) Magnetic properties of soils from sites with different geological and environmental settings. J Appl Geophys 59:273–283

Goktepe AB, Altun S, Sezer A (2005) Soil clustering by fuzzy c-means algorithm. Adv Eng Softw 36(10):691–698

Han J, Kamber M (2006) Data mining, concepts and techniques. Morgan Kaufman Publishers, San Francisco

Hanesch M, Scholger R (2002) Mapping of heavy metal loadings in soils by means of magnetic susceptibility measurements. Environ Geol 42:857–870

Hanesch M, Scholger R (2005) The influence of soil type on the magnetic susceptibility measured throughout soil profiles. Geophys J Int 161:50–56

Hanesch M, Rantitsch G, Hemetsberger S, Scholger R (2007) Lithological and pedological influences on the magnetic susceptibility of soil: their consideration in magnetic pollution mapping. Sci Total Environ 382:351–363

Hussein MT (2004) Hydrochemical evaluation of groundwater in the Blue Nile Basin, eastern Sudan, using conventional and multivariate techniques. Hydrogeol J 12:144–158

IUSS Working Group WRB (2007) World reference base for soil resources 2006, first update 2007. World soil resources reports no. 103. FAO, Rome

Jordanova D, Hoffmann V, Fehr KT (2004) Mineral magnetic characterization of anthropogenic magnetic phases in the Danube river sediments (Bulgarian part). Earth Planet Sci Lett 221:71–89

Jordanova D, Jordanova N, Petrov P (2014) Magnetic susceptibility of road deposited sediments at a national scale—relation to population size and urban pollution. Environ Poll 189:239–251

Kapicka A, Petrovsky E, Jordanova N (1997) Comparison of in situ field measurements of soil magnetic susceptibility with laboratory data. Stud Geophys Geod 41(4):391–395

Kapicka A, Petrovksy E, Jordanova N, Podrazsky V (2001) Magnetic parameters of forest top soils in Krkonose Mountains, Czech Republic. Phys Chem Earth A Solid Earth Geod 26:917–922

Kapicka A, Dlouha S, Grison H, Jaksik O, Petrovsky E, Kodesova R (2013) Magnetic properties of soils—a basis for erosion study at agricultural land in southern Moravia. In: Book series: international multidisciplinary scientific GeoConference-SGEM, pp 577–584

Kazakis N, Voudouris K (2015) Groundwater vulnerability and pollution risk assessment of porous aquifers to nitrate: modifying the DRASTIC method using quantitative parameters. J Hydrol 525:13–25

Kazakis N, Voudouris K, Vargemezis G, Pavlou A (2013) Hydrogeological regime and groundwater occurrence in the Anthemountas River basin, northern Greece. Bull Geol Soc Greece XLVII/2:711–720

Kazakis N, Kantiranis N, Vogiatzis D, Pavlou A, Zavridou E (2014) Estimation of saturated hydraulic conductivity with field and empirical methods and the role of sediment maturity. In: Proceedings of the 10th international hydrogeological congress of Greece, Thessaloniki, Oct 2014, vol 1, pp 315–323

Kazakis N, Kantiranis N, Voudouris K, Mitrakas M, Kaprara E, Pavlou A (2015) Geogenic Cr oxidation on the surface of mafic minerals and the hydrogeological conditions influencing hexavelant chromium concentrations in groundwater. Sci of the Total Environ 514:224–238

Kruiver PP, Dekkers MJ, Heslop D (2001) Quantification of magnetic coercivity by the analysis of acquisition curves of isothermal remanent magnetization. Earth Planet Sci Lett 189:269–276

Lecoanet H, Leveque F, Ambrosi J-P (2001) Magnetic properties of salt-marsh soils contaminated by iron industry emissions (southeast France). J Appl Geophys 48:67–81

Ledesma-Ruiz R, Pastın-Zapata E, Parra R, Harter T, Mahlknecht J (2015) Investigation of the geochemical evolution of groundwater under agricultural land: a case study in northeastern Mexico. J Hydrol 521:410–423

Liu QS, Roberts AP, Larrasoaña JC, Banerjee SK, Guyodo Y, Tauxe L, Oldfield F (2012) Environmental magnetism: principles and applications. Rev Geophys 50(RG 4002):1–50

Lu SG, Bai SQ (2006) Study on the correlation of magnetic properties and heavy metals content in urban soils of Hangzhou City, China. J Appl Geophys 60:1–12

Magiera T, Zawadzki J (2007) Using of high-resolution topsoil magnetic screening for assessment of dust deposition: comparison of forest and arable soil datasets. Environ Monit Assess 125:19–28

Magiera T, Strzyszcz Z, Kapicka A, Petrovsky E (2006) Discrimination of lithogenic and anthropogenic influences on topsoil magnetic susceptibility in Central Europe. Geoderma 130:299–311

Magiera T, Kapicka A, Petrovsky E, Strzyszcz Z, Fialova H, Rachwa M (2008) Magnetic anomalies of forest soils in the Upper Silesia-Northern Moravia region. Environ Pollut 156:618–627

Maher B (1986) Characterisation of soils by mineral magnetic measurements. Phys Earth Planet Int 42:76–92

Mountrakis D (1985) Geology of Greece. University Studio Press, Thessaloniki, p 257

Mullins CE (1977) Magnetic susceptibility of the soil and its significance in soil science: a review. J Soil Sci 28:223–246

Pachauri T, Singla V, Satsangi A, Lakhani A, Kumari KM (2013) SEM-EDX characterization of individual coarse particles in Agra, India. Aerosol Air Qual Res 13:523–536

Petrovsky E, Kapicka A (2006) On determination of the Curie point from thermomagnetic curves. J Geophys Res 111:1–10

Petrovsky E, Kapicka A, Zapletal K, Sebestova E, Spanila T, Dekkers MJ, Rochette P (1998) Correlation between magnetic parameters and chemical composition of lake sediments from Northern Bohemia—preliminary study. Phys Chem Earth 23:1123–1126

Petrovsky E, Kapicka A, Jordanova N, Knab M, Hoffmann V (2000) Low-field magnetic susceptibility: a proxy method of estimating increased pollution of different environmental systems. Environ Geol 39:312–318

Rudnick RL, Gao S (2003) Composition of the continental crust. In: Rudnick RL (ed) The crust, treatise on geochemistry. Elsevier, Amsterdam, pp 1–64

Sarris A, Kokkinou E, Aidona E, Kallithrakas-Kontos N, Koulouridakis P, Kakoulaki G, Droulia K, Damianovits O (2009) Environmental study for pollution in the area of Megalopolis Power Plant (Peloponnesus, Greece). Environ Geol 58:1769–1783

Scholger R (1998) Heavy metal pollution monitoring by magnetic measurements applied to sediments of the river Mur (Styria, Austria). Eur J Environ Eng Geophys 3:25–37

Scoullos M, Oldfield F, Thompson R (1979) Magnetic monitoring of marine particulate pollution in the Elefsis Gulf, Greece. Mar Pollut Bull 10:287–291

Strzyszcz Z (1993) Magnetic susceptibility of soils in the areas influenced by industrial emissions. In: Schullin R (ed) Soils monitoring: early detection and surveying of soils contamination and degradation. Birkhauser, Basel, pp 225–269

Thompson R, Oldfield F (1986) Environmental magnetism. Allen and Unwin, London

Thorpe A, Harrison RM (2008) Sources and properties of non-exhaust particulate matter from road traffic: a review. Sci Total Environ 400:270–282

Tissari J, Lyyranen J, Hytonen K, Sippula O, Tapper U, Fre A (2008) Fine particle and gaseous emissions from normal and smouldering wood combustion in a conventional masonry heater. Atm Environ 42:7862–7873

Torrent J, Liu Q, Barrón V (2010) Magnetic susceptibility changes in relation to pedogenesis in a Xeralf chronosequence in northwestern Spain. Eur J Soil Sci 61:161–173. doi:10.1111/j.1365-2389.2009.012.01216x

Verosub K, Roberts AP (1995) Environmental magnetism: past, present, and future. J Geophys Res 100:2175–2192. doi:10.1029/94JB02713

Voudouris K, Lambrakis N, Papatheodorou G, Daskalaki P (1997) An application of factor analysis for the study of the hydrogeological conditions in plio-pleistocene aquifers of NW Achaia (Greece). Math Geol 29(1):43–59

Zananiri I, Kondopoulou D, Spassov S (2010) The application of environmental magnetism techniques for pollution assessment in urban and suburban areas in Greece: State of the art and case studies. Bull Geol Soc Greece 4:1972–1982